

## H<sub>2</sub>O<sub>2</sub>-Replenishable and GSH-Depletive ROS ‘Bomb’ for Self-Enhanced Chemodynamic Therapy

*Fan Zhao,<sup>#,ab</sup> Jing Yu,<sup>#,\*ab</sup> Jiayu Yao,<sup>c</sup> Yu Tong,<sup>c</sup> Dan Su,<sup>d</sup> Qing Xu<sup>ab</sup> Juan Li<sup>ab</sup> Yao Ying,<sup>ab</sup> Wangchang Li<sup>ab</sup> Liang Qiao,<sup>ab</sup> Jingwu Zheng,<sup>ab</sup> Wei Cai,<sup>ab</sup> Xiaozhou Mou,<sup>\*,c</sup> and Shenglei Che,<sup>\*,ab</sup>*

*a College of Materials Science and Engineering, Zhejiang University of Technology, Hangzhou 310014, China*

*b Research Center of Magnetic and Electronic Materials, Zhejiang University of Technology, Hangzhou 310014, China*

*c Clinical Research Institute, Zhejiang Provincial People’s Hospital, Hangzhou 310014, China*

*d Department of Oncology, First Affiliated Hospital of Zhejiang University, Hangzhou 310003, China*

**Table S1.** The content of Fe in CaO<sub>2</sub>-Fe NPs with different feeding ratios

Feeding ratios	Fe (wt%)
10:1	1.1
8:1	2.6
6:1	3.2
4:1	4.0
2:1	-

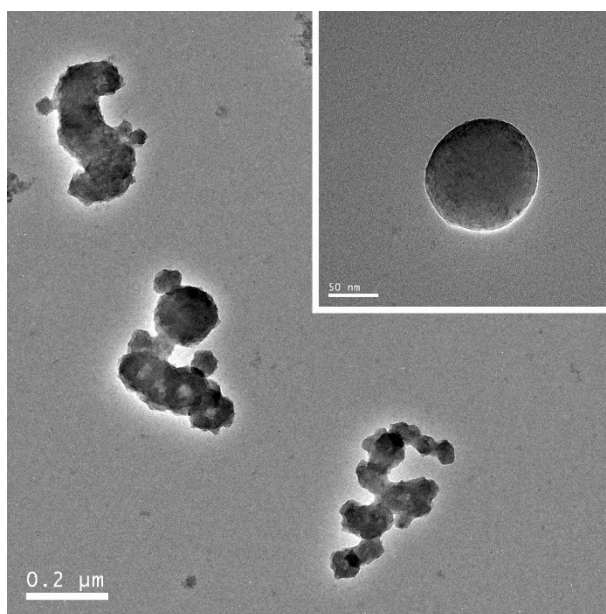


**Figure S1.** TEM image of CaO<sub>2</sub> NPs (inset: an image at a higher magnification of CaO<sub>2</sub> NPs).

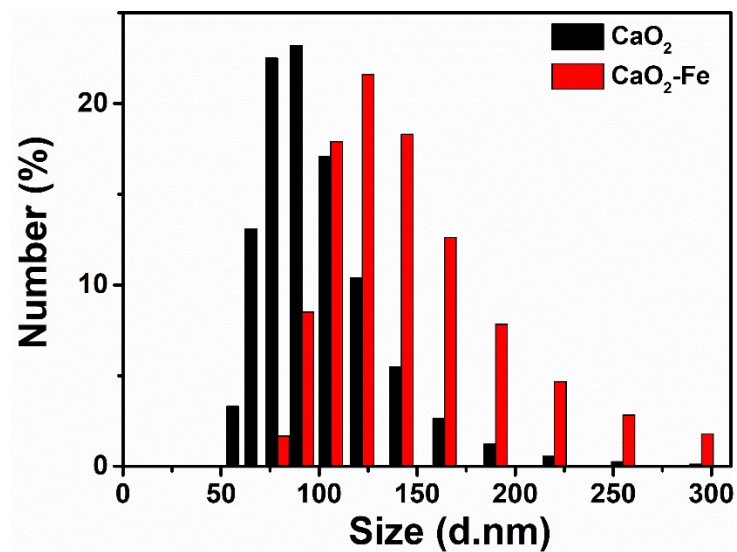


**Figure S2.** Dynamic light scattering (DLS) measurement of CaO<sub>2</sub> and CaO<sub>2</sub>-Fe NPs.

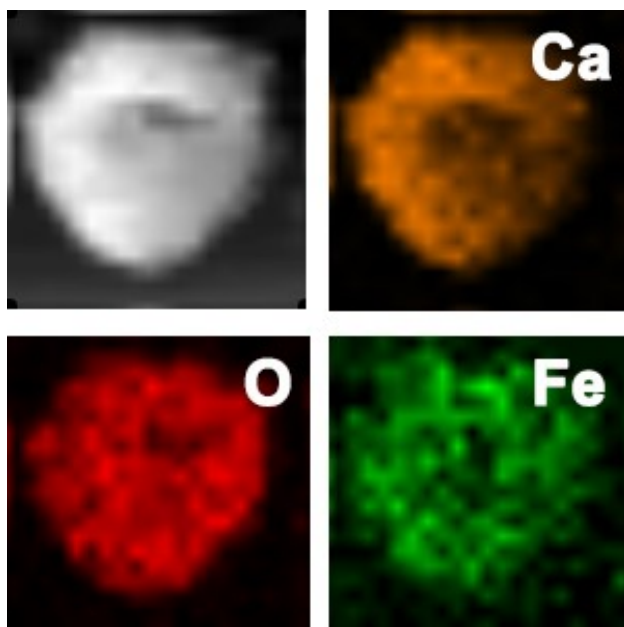


**Figure S3.** HAADF-STEM and elemental mapping of Fe, Ca, and O of CaO<sub>2</sub>-Fe NPs.

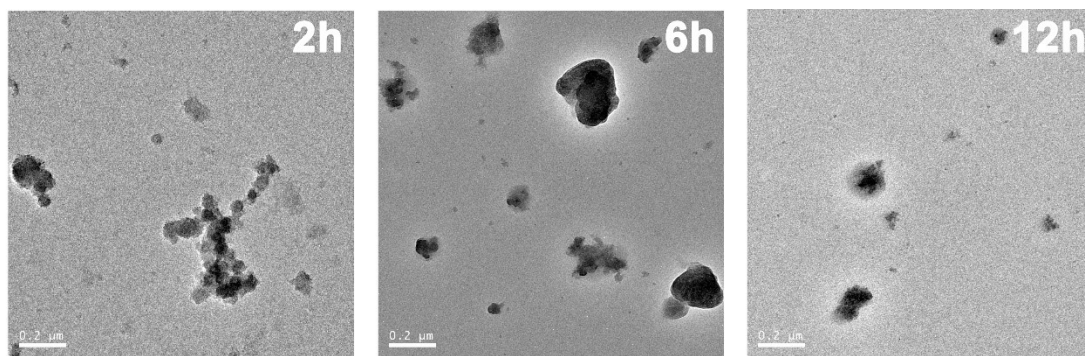


**Figure S4.** TEM image of CaO<sub>2</sub>-Fe NPs by dispersing in pH 5.4 with different time.

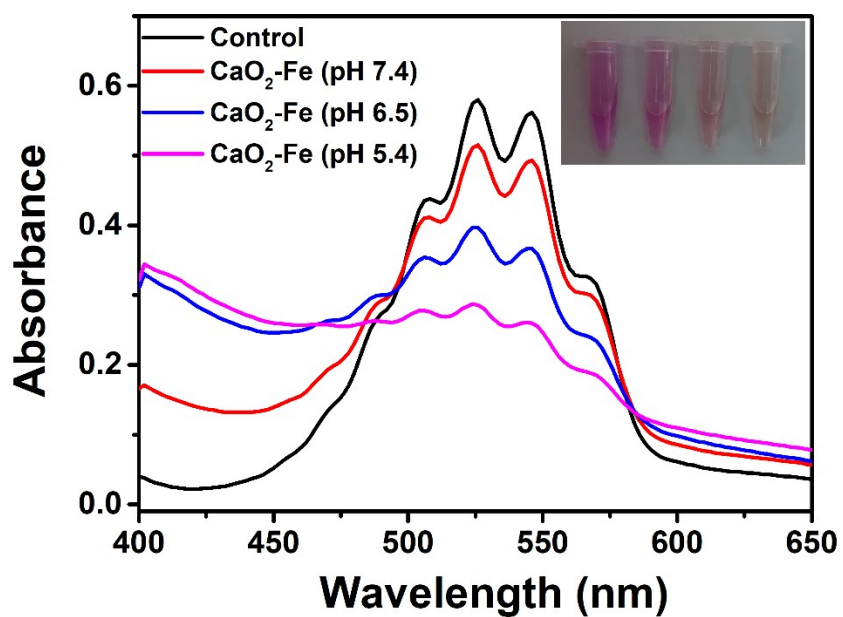


**Figure S5.** UV-Vis absorption spectra and photo (inset) of KMnO<sub>4</sub> after treating with CaO<sub>2</sub>-Fe NPs in different pH environment.

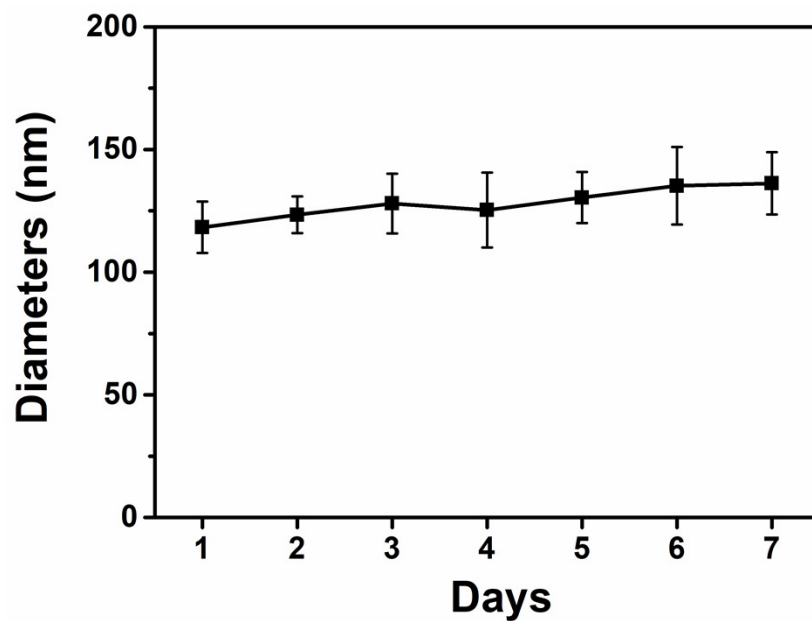


Figure S6. DLS spectrum of CaO<sub>2</sub>-Fe NPs dispersing in PBS with different time.

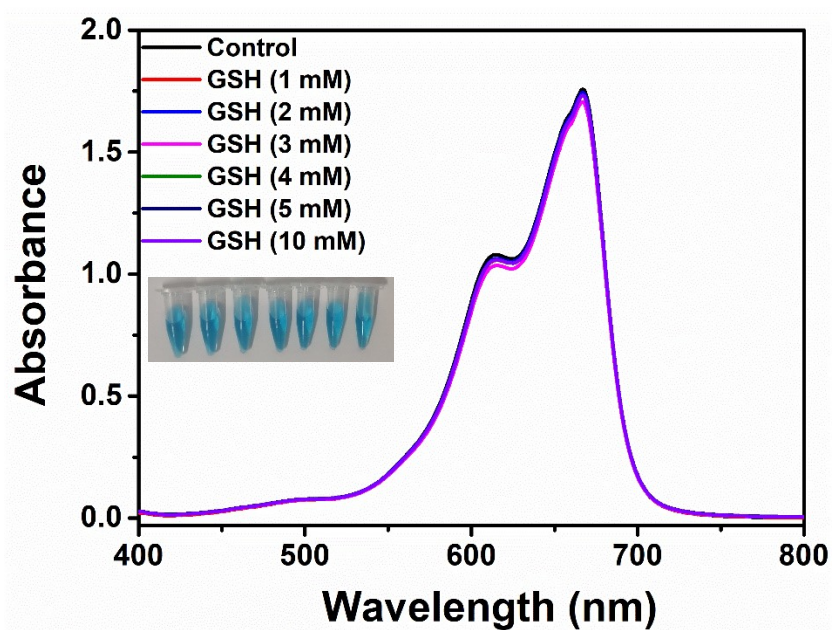
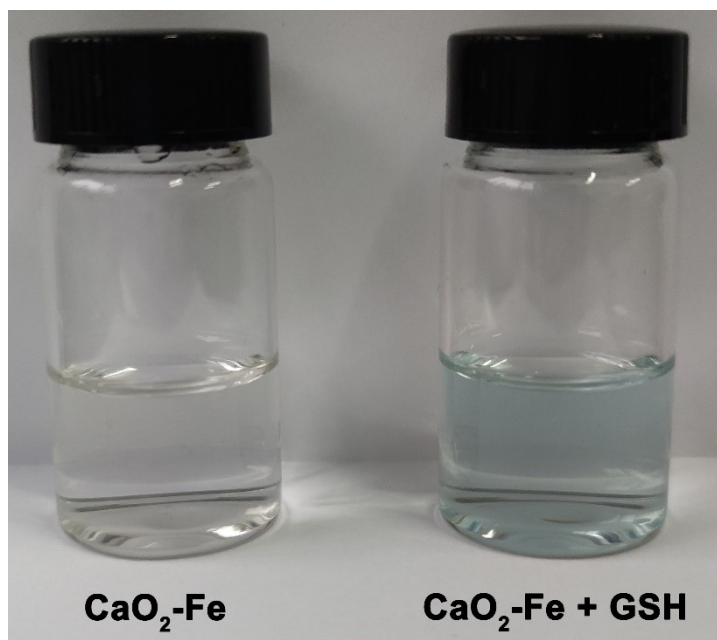
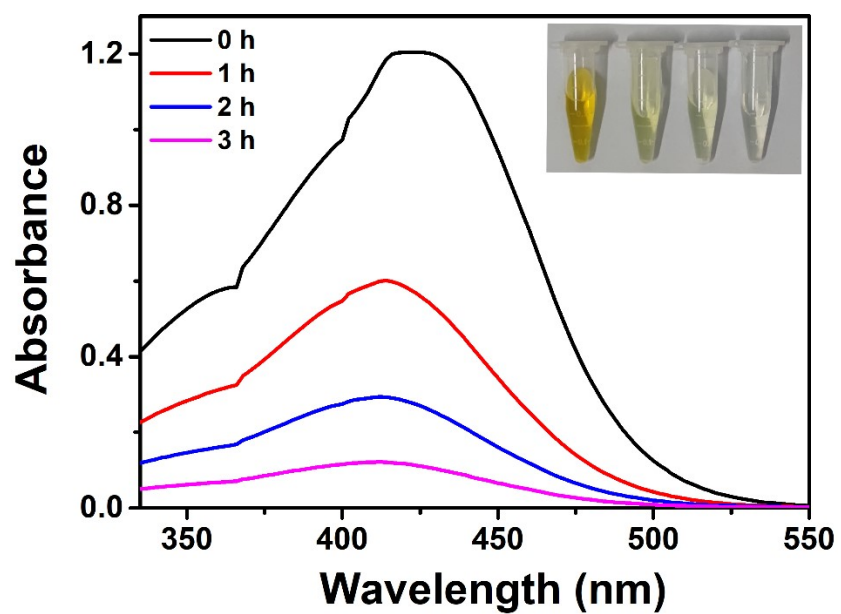


Figure S7. UV-Vis absorption spectra and photo (inset) of MB after degradation by different amount of GSH at pH 5.4.



**Figure S8.** Photos of potassium ferricyanide ( $\text{Fe}^{2+}$  indicator) dispersed in  $\text{CaO}_2\text{-Fe}$  or  $\text{CaO}_2\text{-Fe}$  plus GSH solution.



**Figure S9.** UV-vis absorption spectra and photo (inset) of DTNB (GSH indicator) after treating with  $\text{CaO}_2\text{-Fe}$  NPs and GSH at pH 5.4 in different time.



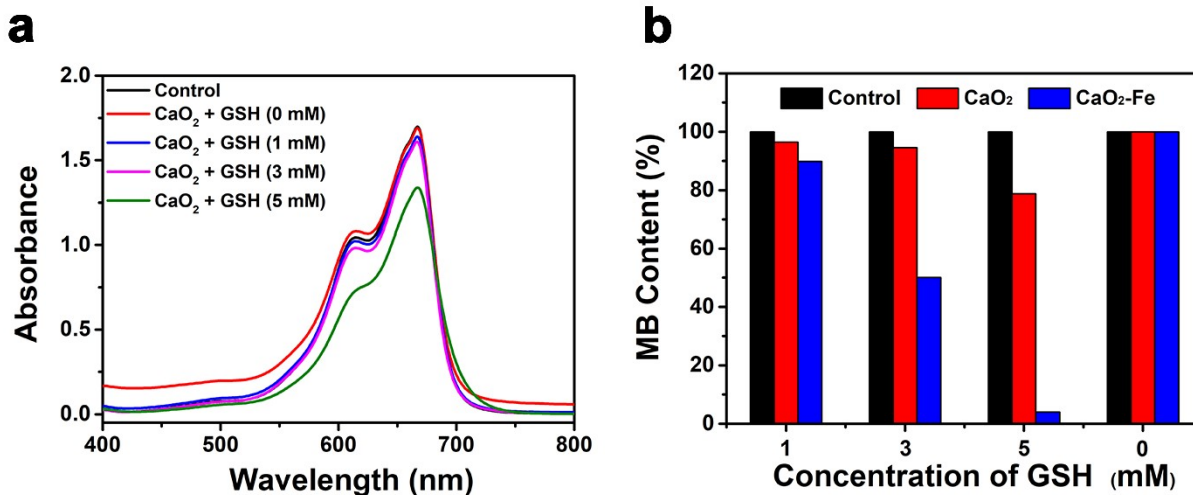


**Figure S10.** (a) UV-Vis absorption spectra of MB after degradation by CaO<sub>2</sub> NPs treated with different amount of GSH at pH 5.4. (b) Bar graph of the degradation percent of MB by CaO<sub>2</sub>-Fe NPs or CaO<sub>2</sub> NPs treated with different amount of GSH at pH 5.4.

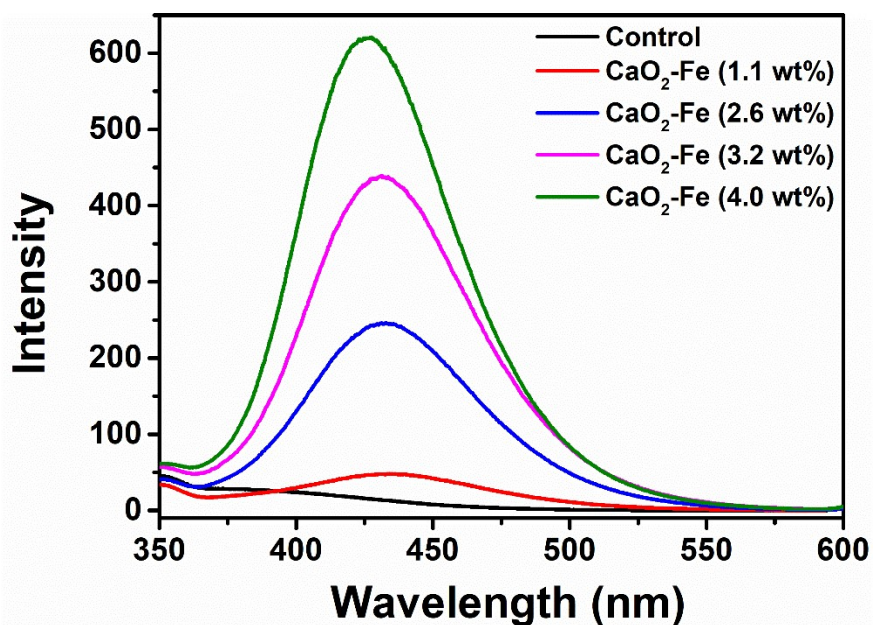


**Figure S11.** TPA assay of CaO<sub>2</sub>-Fe NPs with different Fe (wt%) in pH 5.4 solution with 10 mM GSH.

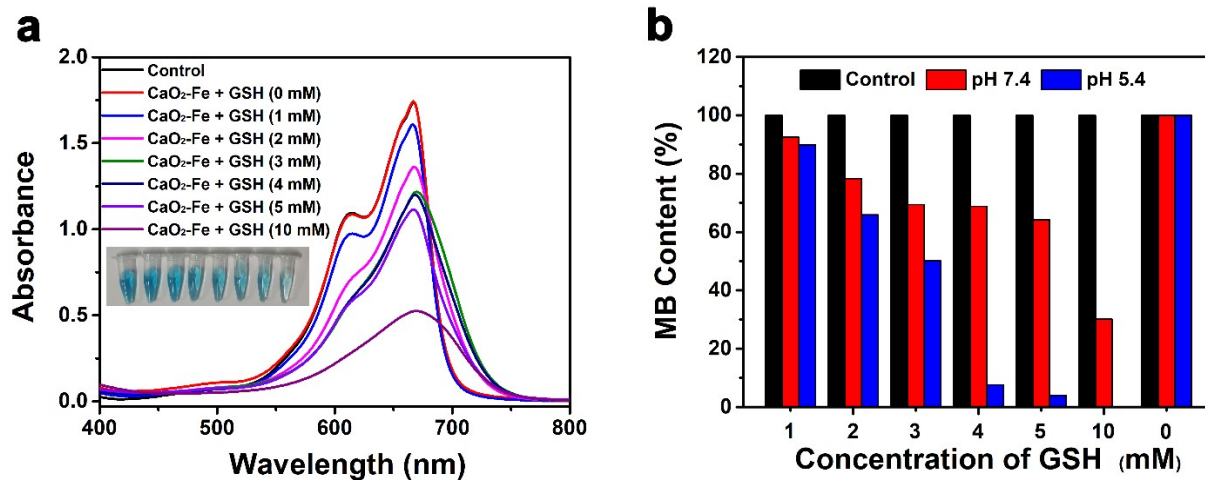


**Figure S12.** (a) UV-Vis absorption spectra and photo (inset) of MB after degradation by CaO<sub>2</sub>-Fe NPs treated with different amount of GSH at pH 7.4. (b) Bar graph of the degradation percent of MB by CaO<sub>2</sub>-Fe NPs treated with different amount of GSH at different pH values.

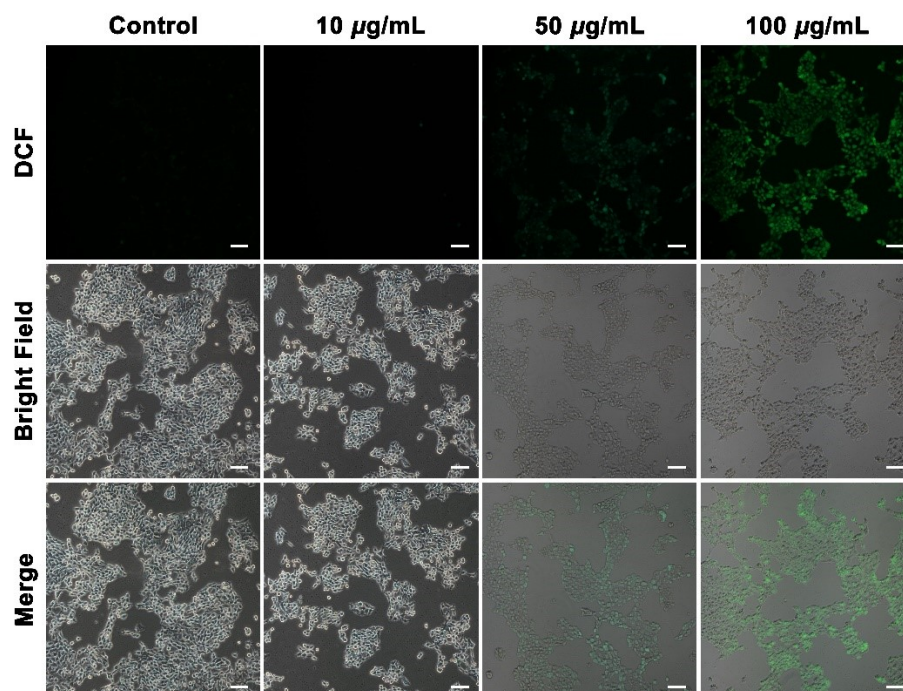


**Figure S13.** Fluorescence images of DCFH-DA-stained 4T1 cells after exposure to different amount of CaO<sub>2</sub>-Fe NPs for 4 h. The scale bar represents 100 μm.



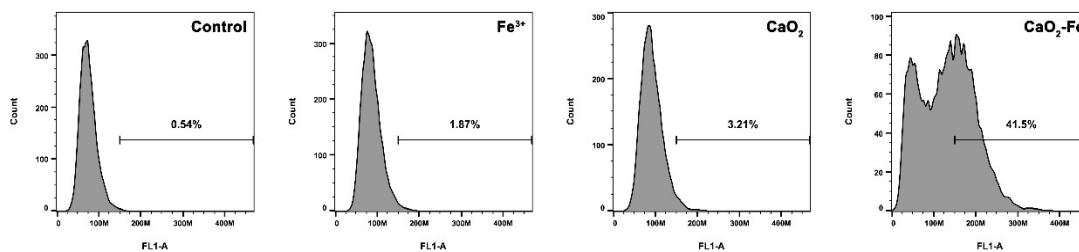


**Figure S14.** Flow cytometry analysis of ROS generation in 4T1 cells treated with different agents, as detected with DCFH-DA.

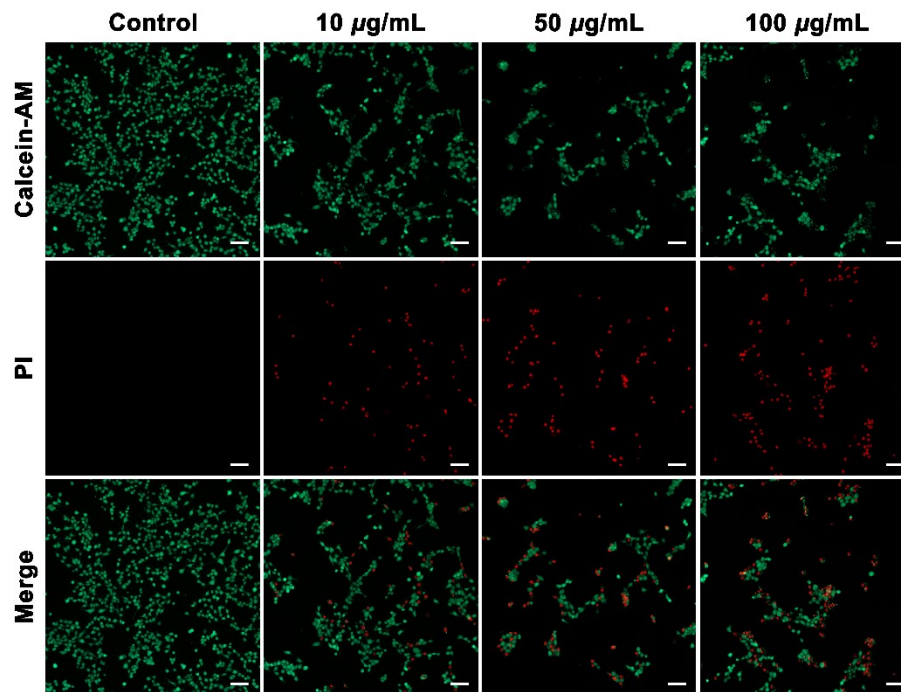


**Figure S15.** Fluorescence images of calcein AM (green, live cells) and PI (red, dead cells) costained 4T1 cells after incubation with different amount of  $\text{CaO}_2\text{-Fe}$  NPs for 24 h. The scale bar represents 100  $\mu\text{m}$ .

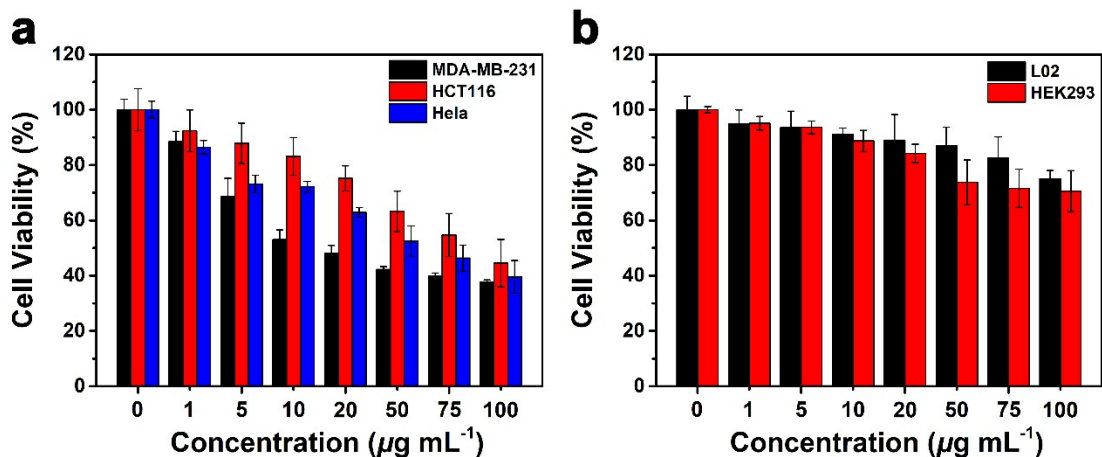


**Figure S16.** (a) Viability of tumor cell lines (HCT 116, MDA-MB-231, and HeLa) after 24 h of incubation with  $\text{CaO}_2\text{-Fe}$  NPs. (b) Viability of normal cell lines (L02 and HEK 293) after 24 h of incubation with  $\text{CaO}_2\text{-Fe}$  NPs.

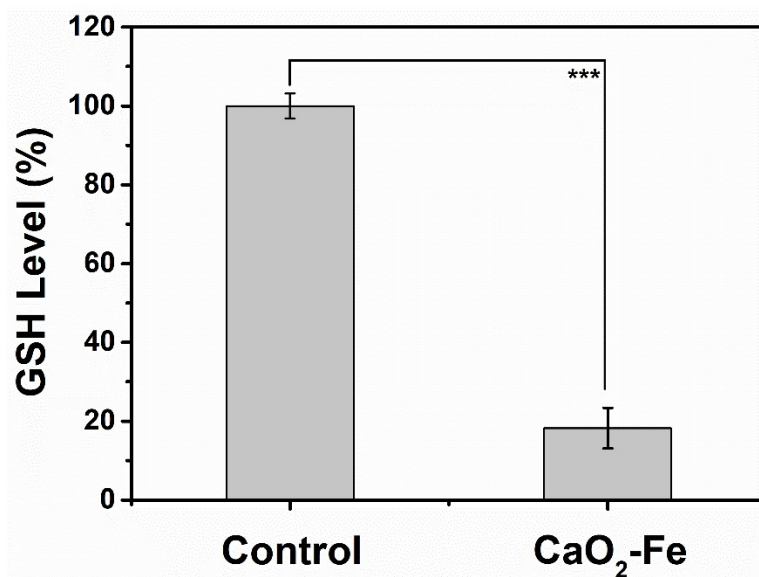


**Figure S17.** Intracellular GSH levels of 4T1 cells after treating with  $\text{CaO}_2\text{-Fe}$  NPs 8h. ( $n = 3$ , mean  $\pm$  s.d., \*\*\* $p < 0.001$ )

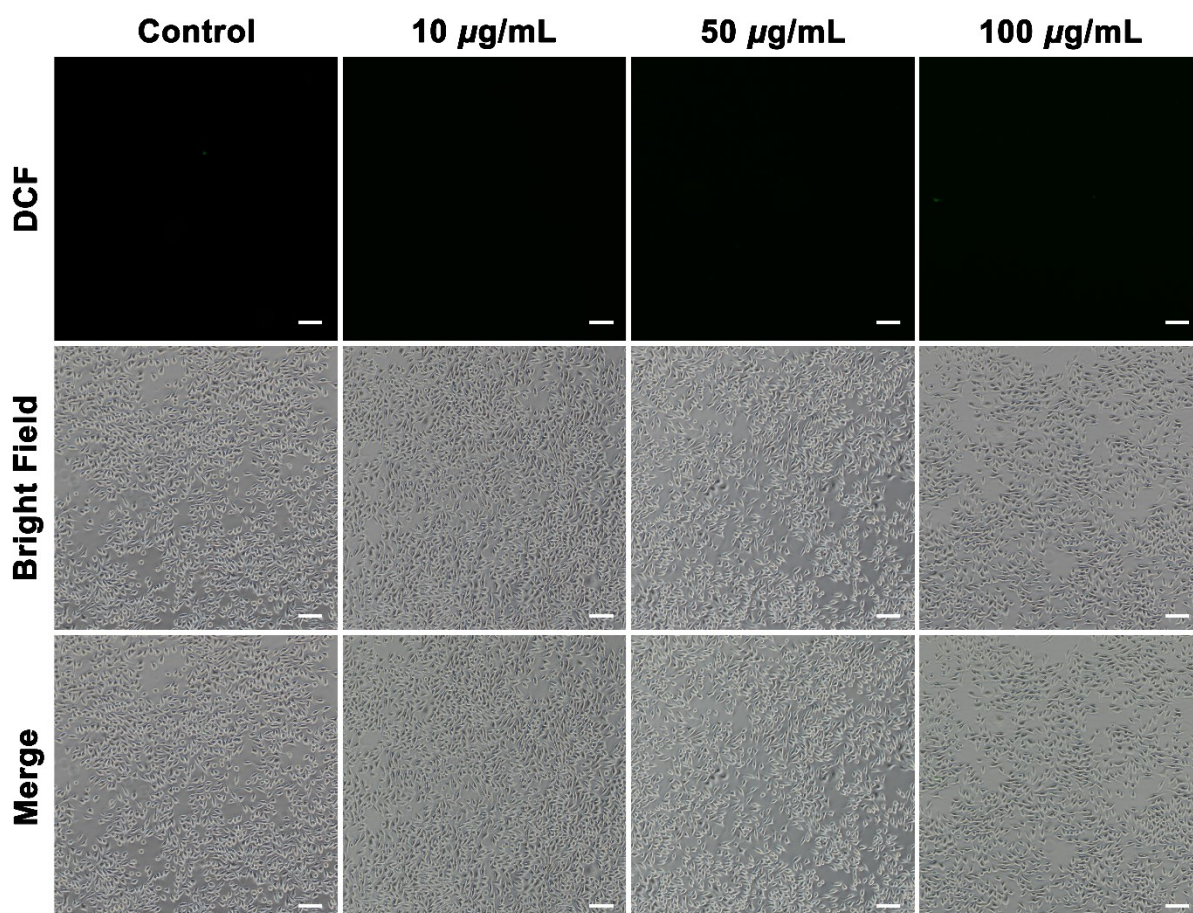


**Figure S18.** Fluorescence images of DCFH-DA-stained L929 cells after exposure to different amount of  $\text{CaO}_2\text{-Fe}$  NPs for 4 h. The scale bar represents 100  $\mu\text{m}$ .

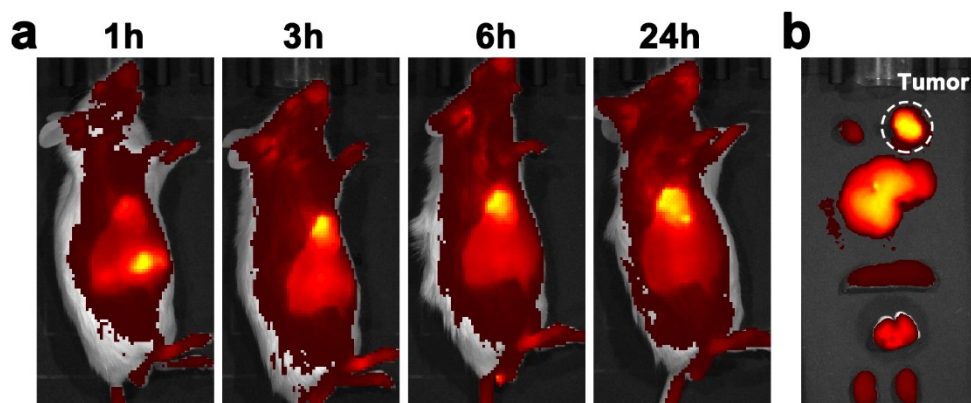


**Figure S19.** (a) In vivo NIR imaging of tumor-bearing mice intravenous injected with IR783-loaded  $\text{CaO}_2\text{-Fe}$  NPs at 1, 3, 6, and 24 h post-injection. (B) NIR imaging of various tissues at 24 h postinjection.



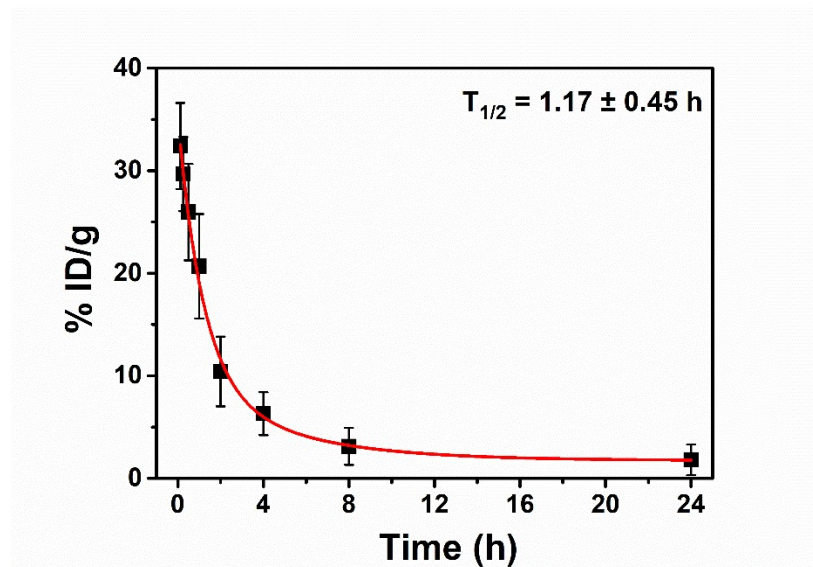


**Figure S20.** Blood circulation of CaO<sub>2</sub>-Fe NPs. The data were obtained by measuring IR-783 fluorescence in the blood samples.

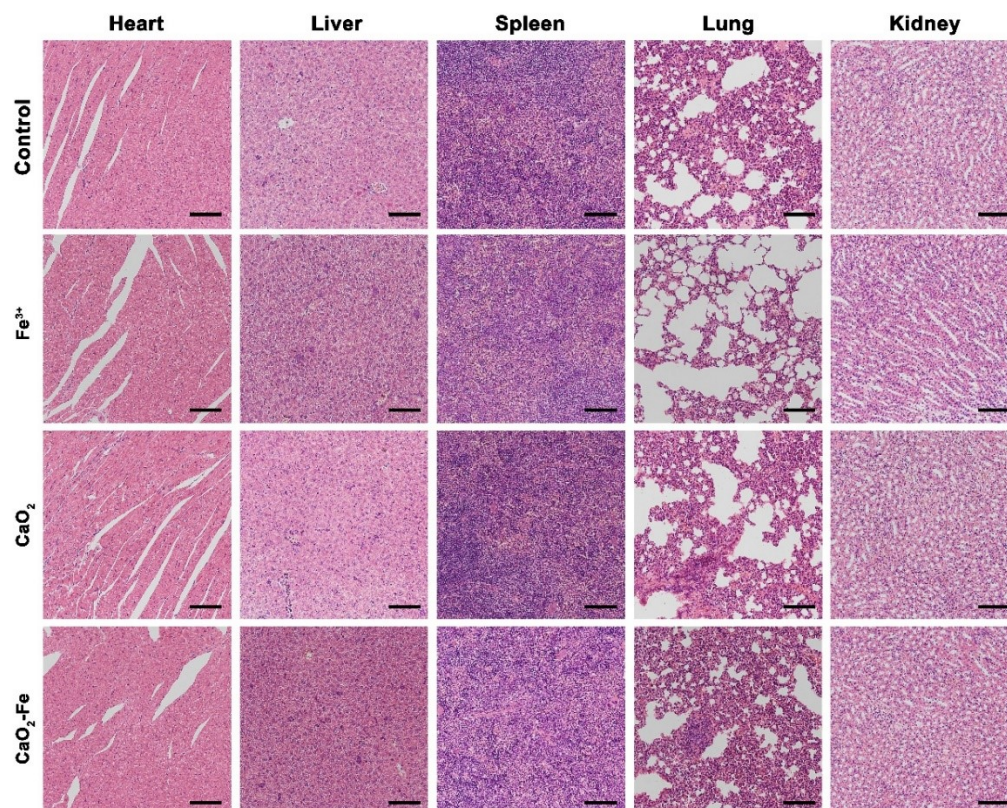


**Figure S21.** Images of H&E stained major tissues after therapy. The scale bar represents 100 μm.

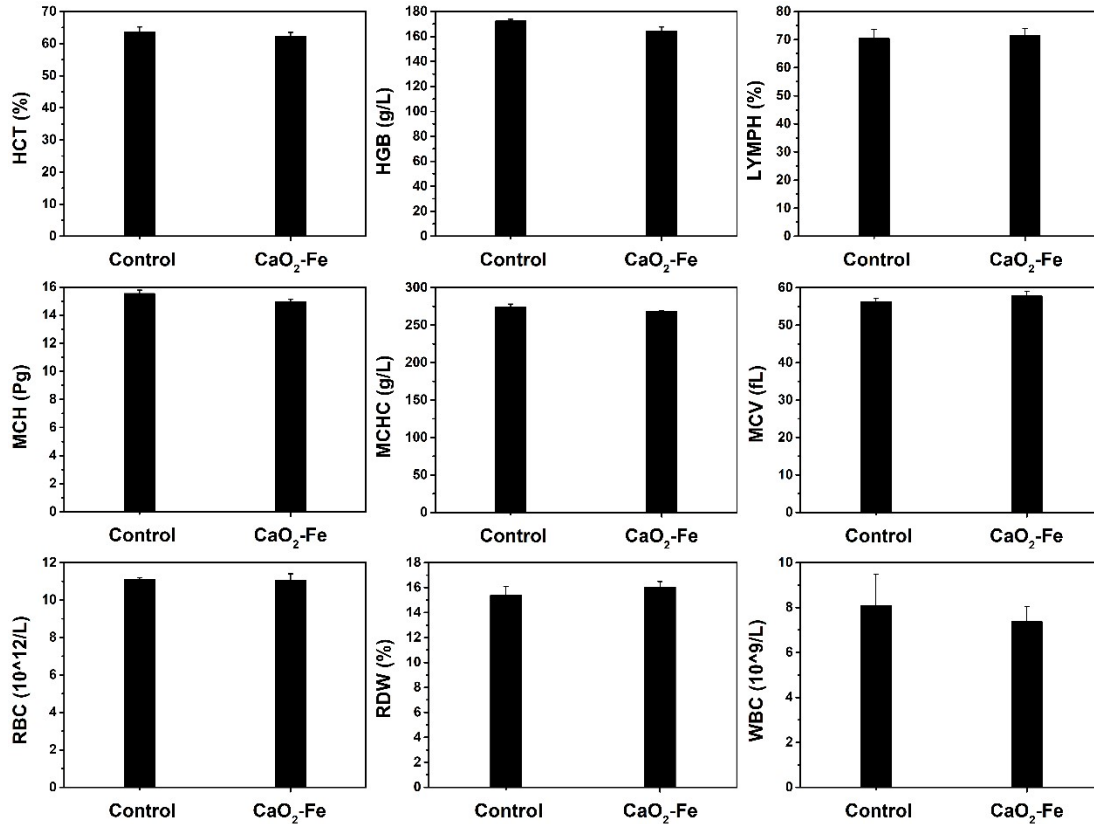


**Figure S22.** Blood hematology analysis of healthy mice after intravenously injected with saline or CaO<sub>2</sub>-Fe NPs for 17 days. (n = 3, mean ± *s.d.*)